Plastocyanin Binding to Photosystem I as a Function of the Charge State of the Metal Ion: Effect of Metal Site Conformation†

Eva Danielsen,*,‡ Henrik Vibe Scheller,§ Rogert Bauer,‡ Lars Hemmingsen,‡ Morten Jannik Bjerrum,|| and Örjan Hansson⊥

Departments of Mathematics and Physics, Plant Biology, and Chemistry, Royal Veterinary and Agricultural University, Thorvaldsensvej 40, DK-1871 Frederiksberg C, Denmark, and Biochemistry and Biophysics, Department of Chemistry, Göteborg University, P.O. Box 462, SE-413-90 Göteborg, Sweden

Received April 15, 1999; Revised Manuscript Received June 7, 1999

ABSTRACT: The binding of Ag- and Cd-substituted plastocyanin to reduced photosystem 1 of spinach has been studied through the rotational correlation time of plastocyanin measured by the technique of perturbed angular correlation of γ-rays (PAC). Ag and Cd are used as models for native Cu(I) and Cu(II), respectively. A dissociation constant of 5 μM was found for Ag-plastocyanin, whereas the dissociation constant was at least 24 times higher for Cd-plastocyanin. PAC was further used to characterize the structure of the metal site of Cd- and Ag-plastocyanin. The Cd spectra are characteristic of a planar configuration of one cysteine and two histidines. However, the spectra show an unusual peak broadening and a high degree of internal motion, interpreted as motion of one of the histidines within the plane. ^{111}Ag decays to ^{111}Cd, followed by the emission of two γ-rays used for the PAC experiment. The ^{111}Ag PAC spectra indicate that one of the coordinating histidines has a different position in the Ag protein than in the Cd protein but that the decay of Ag to Cd causes a relaxation of the position of this histidine to the position in the Cd protein within 20 ns. Binding of Ag-plastocyanin to photosystem I stabilized the Ag metal site structure so that no relaxation was observed on a time scale of 100 ns. This stabilization of the Ag structure upon binding indicates that the metal site structure is involved in regulating how the dissociation constant for plastocyanin depends on the charge of the metal ion.

Plastocyanin is a blue copper protein of about 10 kDa functioning as an electron carrier from cytochrome b_6/f to photosystem I (PSI)[1] in chloroplasts and cyanobacteria. The binding of plastocyanin to PSI as a function of the charge state of the metal ion is thus central for the photosynthetic electron transport. Studies of the absorbance of P700 after a short flash have shown that in higher plants the reduction of photooxidized P700 by plastocyanin is biphasic (*1*−*9*). The fast component of 10−15 μs is in a simple model thought to represent an intracomplex electron transfer of already bound plastocyanin, and the slower phase is thought to represent a bimolecular reaction of plastocyanin and PSI. However, even at very high concentrations of plastocyanin the fast phase is still only about 75% of the total absorbance change and the slow phase saturates with a limiting time constant of about 50−100 μs (*1*−*9*). These discrepancies cannot be explained by the simple model, and more elaborate models have been proposed. A model where the binding of plastocyanin to the PSI complex must be followed by an intracomplex conformational change or rearrangement prior to electron transfer was first proposed by Bottin and Mathis (*6*) and has been further developed in several papers (*1*−*5*, *7*, *9*). Another model has been proposed by Drepper et al. (*8*) where the deviations from the simple model are explained from differences in the reduction potentials for the bound and unbound plastocyanin.

The process of electron transfer from reduced plastocyanin (pc^I) to $P700^+$ can be divided into the following three steps (with the change of free energy in each step indicated):

$$P700^+ + pc^I \xrightleftharpoons{k_B T \ln(K_D^{I,+})} P700^+ \cdot pc^I \xrightleftharpoons{\Delta G^\circ = -e\Delta E_m(\text{complex})} P700 \cdot pc^{II} \xrightleftharpoons{-k_B T \ln(K_D^{II})} P700 + pc^{II}$$

In the reaction scheme originally proposed by Bottin and Mathis (*6*), the first step also involves a conformational change. The total process is simply the reduction of $P700^+$ and oxidation of plastocyanin and therefore the total energy difference, $\Delta G_{tot} = e\,[E_m(pc) - E_m(P700)]$, where $E_m(P700)$ and $E_m(pc)$ denote the reduction potential of free P700 and free plastocyanin, respectively. ΔG_{tot} amounts to approximately −120 millielectron volts (*8*). (We will use the unit of millielectron volts per molecule for the free energy in the

† This work was supported by The Danish Natural Science Research Council via the Center for Bio-inorganic Chemistry, by The Danish Plant Biology Research Center, and by The Swedish Natural Science Research Council.

* Corresponding author (telephone +45 3528 2363; Fax +45 35282350; E-mail eda@kvl.dk).

‡ Department of Mathematics and Physics, Royal Veterinary and Agricultural University.

§ Department of Plant Biology, Royal Veterinary and Agricultural University.

|| Department of Chemistry, Royal Veterinary and Agricultural University.

⊥ Göteborg University.

[1] Abbreviations: NQI, nuclear quadrupole interaction; PAC, perturbed angular correlations of γ-rays; P700, reaction center of photosystem I; PSI, photosystem I.

10.1021/bi990869y CCC: $18.00
Published on Web 08/13/1999

following in order to make the comparison to the reduction potentials simple.) The changes in free energy of the first and the last processes are given by $+k_BT \ln (K_D^{I,+})$ and $-k_BT \ln (K_D^{II})$, respectively (where k_B is Boltzmann's constant, $K_D^{I,+}$ denotes the dissociation constant, of reduced plastocyanin for oxidized P700, and K_D^{II} denotes the dissociation constant of oxidized plastocyanin for reduced P700). The changes in the free energy of the middle step $\Delta G^\circ = -e\Delta E_m$, where ΔE_m is the driving force of the electron transfer in the complex. Thus $\Delta G^\circ - \Delta G_{tot} = \Delta(\Delta G)$ is related to the dissociation constants by the relationship $\Delta(\Delta G) = k_BT \ln (K_D^{II}/K_D^{I,+})$. From this relationship it is clear that a weaker binding of oxidized plastocyanin to P700 than of reduced plastocyanin to $P700^+$ has the price of reducing the driving force for the electron transfer within the complex.

One problem that arises when the dissociation constants are compared to the driving force is that usually K_D^I is measured instead of $K_D^{I,+}$ (K_D^I denotes the dissociation constant of reduced plastocyanin for reduced P700). These two are only the same if the reduction potential of P700 is independent of whether it is binding reduced plastocyanin. For the sake of simplicity we will assume this in the following, bearing in mind that this assumption might not hold true and could further complicate matters.

Drepper et al. (*8*) investigated the dissociation constant of copper-plastocyanin in a number of ways. One approach was based on the ratio K_D^{II}/K_D^I. They found that the dissociation constants depended on the PSI preparation by up to a factor of 5. For the samples showing the strongest binding, which had a ratio of chlorophyll *a* to chlorophyll *b* of 10, they found a K_D^I of 7 μM. The dissociation constant of Cu(II)-plastocyanin was 40 μM, implying a $k_BT \ln (K_D^{II}/K_D^I) = 41$ meV. In a second approach, Drepper et al. (*8*) measured the reduction potential of plastocyanin covalently bound to reduced PSI. This changed the reduction potential of plastocyanin from 360 mV for the free plastocyanin to 410 mV for the bound plastocyanin. The reduction potential of P700 bound to oxidized plastocyanin was measured to be 475 mV and was close to that found for PSI without bound plastocyanin (*8*). Thus, if it is assumed that the reduction potential of P700 is also unaffected by the binding to reduced plastocyanin, then $\Delta(\Delta G)$ is approximately 55 meV. The third approach is based on the effect of the reduced driving force on the equilibrium distribution of the electron at plastocyanin and at P700, respectively. This offers a possible explanation of the observation that the fast component of the absorbance change saturates at 75%. If all of the limited saturation is explained by the reduced driving force, then a limiting saturation at 75% would imply a driving force of 28 mV corresponding to a $\Delta(\Delta G)$ of 92 mV. One possible source for these variations is the assumption that $K_D^I = K_D^{I,+}$ (equivalent to the reduction potential of P700 being independent of whether it is bound to reduced plastocyanin). Another important aspect that has been ignored in this comparison is the conformational change suggested by Bottin and Mathis (*6*), which could also contribute to the saturation of the fast component.

The differences between the two models make it desirable to investigate the binding of plastocyanin to reduced PSI by a different method, which can also in the future be used to investigate the binding to oxidized PSI. In the present paper the binding between plastocyanin and PSI is studied by PAC spectroscopy after the copper ion of spinach plastocyanin is substituted with radioactive ^{111m}Cd or ^{111}Ag.

PAC spectroscopy measures the nuclear quadrupole interaction (NQI) of a nucleus in the intermediate state of a $\gamma-\gamma$ cascade. ^{111}Ag decays to an excited state in ^{111}Cd before the $\gamma-\gamma$ cascade. Thus for both isotopes used in the present study, ^{111m}Cd and ^{111}Ag, the intermediate level is the excited spin $^5/_2$ state of ^{111}Cd. In the presence of an electric field gradient, a specific coordination geometry will result in three peaks in the Fourier transformed PAC spectrum, referred to as the first, second, and third angular frequencies. From the position and amplitude of these three peaks the two major NQI parameters $\omega_\perp$ and $\omega_\parallel$ can be determined uniquely by the relations given elsewhere (*10*). The method is described in detail in the review by Frauenfelder and Steffen (*11*) and with special emphasis on biological application by Bauer (*12*). An introduction to the technique applied to proteins containing metal ions is given by Bauer et al. (*13*).

The structure of oxidized plastocyanin has been determined for poplar plastocyanin (*14*), spinach plastocyanin (*15*), and reduced poplar plastocyanin (*16)*. For oxidized plastocyanin the copper ion is coordinated to His37, His87, and Cys84, and axial to this plane at a distance of 2.9 Å from the copper ion is S(Met92). For reduced poplar plastocyanin at high pH the copper ion coordinates to the same amino acids, but at low pH (pH 3.8) His87 is protonated and the imidazole ring is rotated by 180° about $C^\beta-C^\gamma$. In this conformation the copper ion is instead coordinated to His37, Cys84, and Met92.

The metal site structure of the blue copper protein azurin has been studied in detail by ^{111m}Cd and ^{111}Ag PAC (*17*−*19*). Comparison of wild-type spectra and spectra of mutant proteins together with model calculations show that Cd and Ag in wild-type azurin are both three-coordinated in a planar and very rigid conformation to two histidines and one cysteine in accordance with the structure of the copper protein (*20*, *21*). As shown in the present study, Cd and Ag in plastocyanin also coordinate to two histidines and one cysteine. Such a conformation is known to result in a value of $\omega_\perp$ that is independent of the angular position of the ligands in the plane but will decrease if the metal ion is shifted out of the plane (*18*). The other major parameter, $\omega_\parallel$, depends on the angles between the histidines and the cysteine in such a way that a smaller angle between the histidines will increase the value of $\omega_\parallel$. It has previously been shown by Tröger et al. (*22*) that plastocyanin possess an unusual spectroscopic characteristic in the Cd PAC spectrum, where the second and third line in the spectrum are much wider than the first line. In the present paper we elaborate more on the dynamics behind and structural significance of these characteristics and include studies of Ag-plastocyanin. These studies, which supply structural information of the copper site in plastocyanin, also serve as the background for the studies of the binding of Ag-plastocyanin and Cd-plastocyanin to PSI.

There are several advantages of using the PAC technique for studying the binding of plastocyanin to PSI in supplement to the traditional technique, where the interaction between plastocyanin and PSI is investigated by the absorbance changes due to P700 rereduction following a short flash: First, the binding observed by PAC is not influenced by the electron transfer pathways. Second, the dissociation constant

can be determined independently for the two different charge states of the metal ion, where the traditional way determines the binding of Cu(II)-plastocyanin to PSI through competition with the binding of Cu(I)-plastocyanin to PSI and is observed by the prevention of the functional electron transfer within the complex formed by plastocyanin and PSI. Third, PAC gives information about conformational changes at the metal site of plastocyanin. It is thus possible to observe differences in the metal site structure between the monovalent Ag ion and the divalent Cd ion. If the structural difference relaxes on a time scale of 10−100 ns, as in the present case, then the relaxation time as well as the structural difference is observable.

MATERIALS AND METHODS

Preparation of ^{111m}Cd and ^{111}Ag. ^{111m}Cd has a half-life of 48.6 min and decays through the emission of two successive γ-rays to the ground state of ^{111}Cd. ^{111}Ag has a half-life of 7.5 days and decays to ^{111}Cd by a β^- decay. Only about 0.2% of these decays result in the successive emission of two γ-rays suitable for PAC spectroscopy. It is important to note that although we refer to the experiments and spectra as Ag PAC and Ag spectra, the two γ-rays are emitted from Cd. The excited level in ^{111}Cd that is populated by the β^- decay of ^{111}Ag has a half-life time of 27 ps. This is enough time to adjust the electronic structure but, as previously shown, not always enough to adjust the molecular structure to that of the Cd protein (*19*, *23*).

^{111m}Cd was produced by bombarding ^{108}Pd with α-particles at the cyclotron at the National Hospital, Copenhagen, Denmark. The ^{111m}Cd was separated from the palladium by the procedure previously described (*13*). ^{111}Ag was produced by neutron irradiation for 7 days of 99.99% pure palladium foil or palladium powder enriched in ^{110}Pd to 98.64%. In the latter case a smaller amount of palladium could be used and therefore the palladium could be dissolved in a smaller amount of aqua regia after the neutron activation. Otherwise the ^{111}Ag was separated from the palladium by the procedure previously described (*19*).

Preparation of PSI. Spinachia oleracea L. was obtained from a local market and PSI was isolated by use of the detergent *n*-decyl β-maltopyranoside according to the previously described procedure (*24*, *25*). The PSI complex obtained after sucrose gradient centrifugation was concentrated by ultracentrifugation at 196000*g* for 22 h and the resulting pellet was resuspended in 25 mM Hepes-KOH (pH 8.0) and 0.3% decyl maltoside. PSI prepared in this way has a Chl/P700 ratio of about 200 and shows very high photochemical activity (*24*). P700 was determined chemically from the ferricyanide-oxidized minus ascorbate-reduced difference spectrum with an absorption coefficient at 700 nm of 64 mM^{-1} cm^{-1}. Photochemically active P700 was determined from the flash-induced absorbance change at 834 nm with the setup previously described (*26*) and an absorption coefficient of 5 mM^{-1} cm^{-1}. No significant difference was found between chemically and photochemically determined P700. Chlorophyll was determined according to Arnon (*27*).

Preparation of Apoplastocyanin. Plastocyanin was isolated from *Escherichia coli* cells transformed with expression plasmids for spinach plastocyanin as described previously (*28*). Apoplastocyanin was prepared by dialysis of 400−750 μL of 1 mM copper-plastocyanin against 5 mL of 0.1 M KCN and 0.1 M Tris, pH 9.5. The KCN was removed by 6-fold dialysis against 50 mL of 50 mM Hepes, pH 7.5. In each step the buffer was flushed with N_2 before the dialysis bag was transferred to the buffer. The container was closed and the dialysis was carried out at 5 °C. This resulted in an apoprotein that could be reconstituted to 20% as judged by the ability to regain absorbance at 600 nm by copper incubation as well as the ability to bind radioactively labeled Cd. The fraction that was unable to bind metal ions was shown to contain oligomers (predominantly dimers and trimers), possibly formed as a result of the high pH in the KCN procedure. The content of oligomers was determined by running an HPLC separation on a Superdex 200 HR 10/30 column and observing the refraction index (in order to obtain the weight concentration of the protein) as well as light scattering (for monitoring the size of the oligomers). The oligomers were unable to bind metal ions and thus are not believed to interfere with the PAC experiments. No attempts were made to remove the oligomers. The concentrations of plastocyanin listed in Tables 1 and 2 are total plastocyanin concentrations based on the absorbance of the apoplastocyanin at 278 nm. (These concentrations are not used in the calculations of the binding constants since we do not expect apoprotein to bind to PSI and the concentration of radioactively labeled plastocyanin is insignificant compared to the PSI concentrations.) The apoprotein was kept frozen at −80 °C until the experiments, when it was quickly thawed before mixing with the aqueous solution of ^{111}Ag or ^{111m}Cd. The incubation time was at least 20 min.

Azurin. One experiment on ^{111m}Cd-substituted azurin from *Pseudomonas aeruginosa* in 55% sucrose was performed as described previously (*17*) but at a temperature of −11 °C. This sample as well as plastocyanin samples at −11 °C were first frozen in liquid nitrogen to ensure that they were in the solid phase.

PAC. The PAC spectrometer consists of six BaF_2 scintillation detectors and is a built-out version of the PAC camera described previously (*29*). The temperature of the sample was controlled within 2 °C by a Peltier element. The experiments were carried out under conditions where P700 is mostly in the reduced state. The perturbation function was formed from the individual coincidence spectra as described previously (*30*).

Angular Overlap Model Calculations. The NQI can be calculated in the angular overlap model, which is a semiempirical molecular orbital model based on observed NQIs for a series of coordination compounds of Cd, based on the assumption that each ligand contributes to the charge distribution in a manner that is independent of the other ligands and with axial symmetry around the metal ion−ligand bond. In the present paper the angular overlap model is only used to give an estimate of the difference in structure between the metal site in Ag-plastocyanin and in Cd-plastocyanin, respectively. Details of the calculations are given elsewhere (*18*).

The angular overlap model calculations of PAC spectra for a planar configuration of one cysteine and two histidines is particularly simple (*18*). Here it suffices to say that for

randomly oriented molecules it is described by the two major diagonal elements of the NQI tensor $\bar{\bar{\omega}}$, ω_{yy} and ω_{zz}, where ω_{yy} is the diagonal element of $\bar{\bar{\omega}}$ for a *y*-axis perpendicular to the plane formed by the three ligands, and ω_{zz} is the diagonal element of $\bar{\bar{\omega}}$ for a *z*-axis almost coinciding with the bond between the cysteine and the metal ion. These two parameters are hereafter denoted $\omega_\perp$ and $\omega_\parallel$, respectively. As mentioned in the introduction, $\omega_\perp$ depends on how close the metal ion is to the plane formed by the three ligands, and $\omega_\parallel$ depends on the Cys−metal ion−His angles.

NQI Determination. The perturbation function $A_2G_2(t)$ was analyzed by conventional least χ^2 fitting routines. Each NQI is described by the parameters $\omega_\parallel$, $\omega_\perp$, $\Delta\omega_\parallel/\omega_\parallel$, $\Delta\omega_\perp/\omega_\perp$, λ, and A_2. The two parameters $\Delta\omega_\parallel/\omega_\parallel$ and $\Delta\omega_\perp/\omega_\perp$ are used for describing small inhomogeneities in the NQI due to variations from one molecule to another with respect to conformations of the probe sites. It was found that, within the uncertainty, $\Delta\omega_\perp/\omega_\perp$ was zero for all samples measured at temperatures above 0 °C. For samples measured at temperatures above 0 °C, the NQIs were therefore described by a single $\omega_\perp$ and a Gaussian distribution of $\omega_\parallel$ with the standard deviation $\Delta\omega_\parallel$ (this parameter was included in the analysis by folding $G_2(t)$ numerically with the distribution in $\omega_\parallel$). This special distribution gives rise to a very narrow first angular frequency (seen as the dominating peaks in Figure 1) and very broad second and third angular frequencies. According to the angular overlap model interpretation of $\Delta\omega_\parallel/\omega_\parallel$, there is a distribution in one of the Cys−metal ion−His angles (vide infra). It should be noted that this way of analyzing the spectra is in contrast to the conventional way, where the frequency distribution results in the same relative width in the three angular frequencies. For the Ag spectra at −11 °C the reduced χ^2 could be improved by including a distribution in $\omega_\perp$ as well. This was done by introducing the conventional frequency-distribution in $G_2(t)$ before the numerical folding (mentioned above) was carried out.

If the rotational diffusion induced by Brownian motions is significant on the time scale of the lifetime of the intermediate state in the PAC isotope (the half-life is 85 ns) but yet slower than the oscillations in the perturbation function, it will cause an exponential damping of the three angular frequencies. This is best observed in the perturbation function before it is Fourier transformed. For slow reorientation the perturbation function is damped by a factor of $\exp(-\lambda t)$, where λ is the inverse of the correlation time of the rotational diffusion, τ_c. As λ approaches the resonance frequencies, as is the case for plastocyanin in aqueous solution at 1 °C, the effect on the perturbation function becomes more complicated and it is necessary to use numerical methods when the data are analyzed (*31*).

The coefficient A_2 gives the amplitude of the anisotropy in the angular correlation between the two γ-rays. A_2 depends only on the nuclear decay and has the value 0.17 for ^{111m}Cd and −0.18 for ^{111}Ag (*32*). In the actual experiments the solid angles of the detectors and the size of the sample result in lower values.

In some of the data analyses of the Cd spectra it was necessary to include unbound Cd. This gives rise to an extra term as an exponential decay in the perturbation function. Including this affected the determination of λ but did not affect the other parameters. The amount included was 5% in the spectrum at 1 °C, 55% sucrose; 11% in the spectrum at 30 °C, 55% sucrose; and 11% in the spectrum in the absence of both sucrose and PSI.

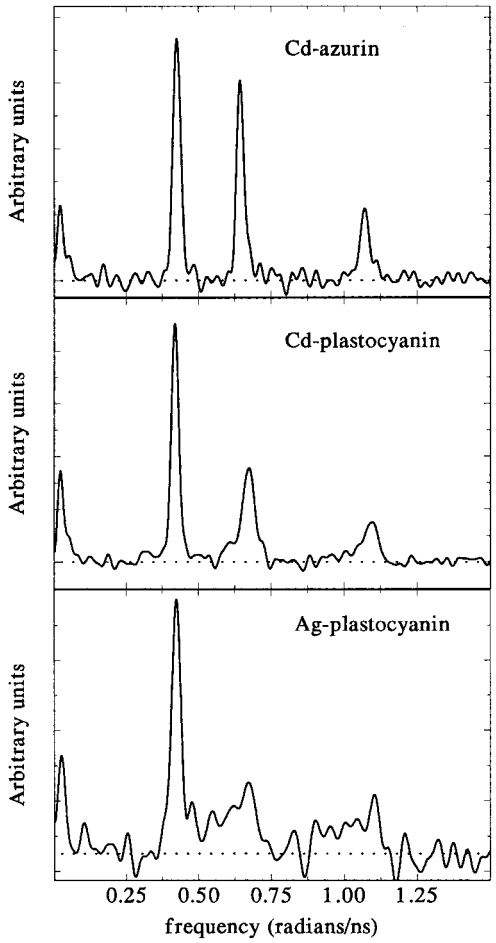

FIGURE 1: (Top panel) Fourier transform (details given in Materials and Methods) of the perturbation function of ^{111}Cd-azurin (*17*). (Middle panel) Fourier transform of the ^{111m}Cd-plastocyanin perturbation function. (Bottom panel) Fourier transform of ^{111}Ag-plastocyanin perturbation function. All three spectra were collected at 1 °C in 55% sucrose. Note that the first angular frequency is almost identical for all three spectra but that the second and third angular frequencies are shifted and broadened for the plastocyanin spectra. For ^{111}Ag this shift depends on the time window used in the Fourier transform, such that the lines are shifted to lower frequencies for data collected immediately after the decay from Ag to Cd. In each spectrum, the baseline is displayed as the dotted horizontal line.

Fourier Transformations. Cosine Fourier transformations were used to compare the measured perturbation function to the calculated perturbation function. All analyses were carried out on the perturbation functions, and the Fourier transforms were used only to guide the analysis. For the spectra displayed in Figure 1 the cosine transforms were carried out on data from 4.5 to 225 ns for the Cd spectra and from 5 to 169 ns for the Ag spectrum. To minimize artifacts arising from not including the first 5 ns, this part of the perturbation function was extrapolated from the data by use of the perturbation function of the best fit. Artifacts from cutting off at 225 ns or 169 ns were taken care of by windowing the data with a Kaiser−Bessel window. As baseline the weighted average of the data was used.

Table 1: NQIs of ^{111}Cd- and ^{111}Ag-Plastocyanin[a]

	experimental conditions	$\omega_{yy} = \omega_{\perp}$ (rad/ns)	$\omega_{zz} = \omega_{\|}$ (rad/ns)	"$\Delta\omega_{\perp}/\omega_{\perp}$" (%)	$\Delta\omega_{\|}/\omega_{\|}$ (%)	λ (ns^{-1})
^{111}Cd	−11 °C, 55% sucrose, 37 mM Tris, pH 7.0	0.2542(2)	0.354(2)	0 (f)	4.4(3)	0.0049(5)
^{111}Cd	1 °C, 55% sucrose, average of several experiments, 28−57 mM Hepes, pH 7.3−7.6	0.2532(2)	0.3484(4)	0 (f)	2.8(1)	0.0063(4)
^{111}Ag	−11 °C, 55% sucrose, 20.2 mM Hepes	0.2540(5)	0.313(2)	1.1(4)	11.8(5)	0.0045(9)
^{111}Ag	1 °C, 55% sucrose, 20.2 mM Hepes	0.2551(5)	0.344(3)	0 (f)	5.9(7)	0.007(1)
^{111}Ag	1 °C + PSI average of two experiments with PSI (see Table 2)	0.262(2)	0.320(7)	0 (f)	8(2)	0.026(6)

[a] Numbers in parentheses denote standard deviations on the least significant digit; an f indicates that the parameter was fixed during the data analysis. Apoplastocyanin concentrations ranged from 5 to 80 μM. Only the part of the Ag spectrum that was collected after 17 ns after the emission of the first γ-ray were included in this analysis.

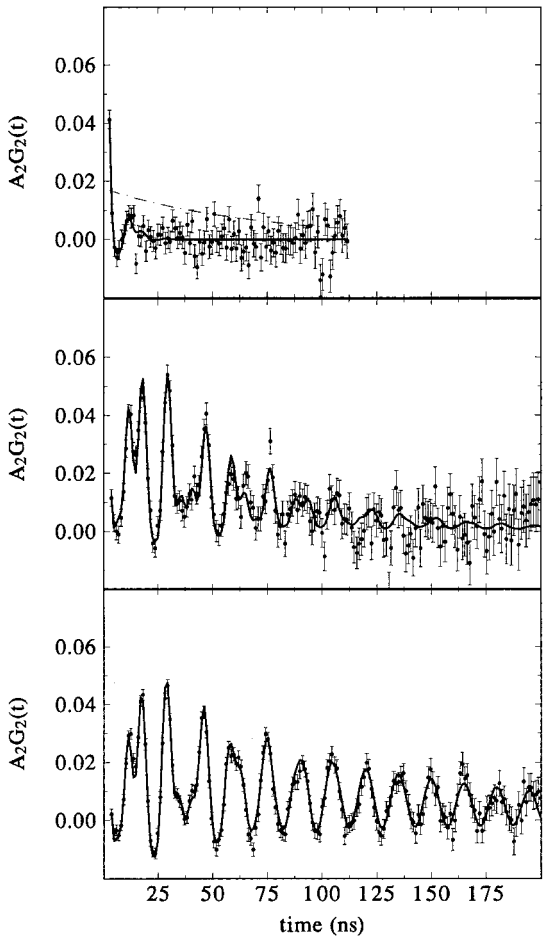

FIGURE 2: Perturbation functions of ^{111m}Cd-plastocyanin for solutions with different viscosities ξ: (top) 1 °C, no sucrose, $\xi = 1.7 \times 10^{-3}$ kg m^{-1} s^{-1}; (middle) 30 °C in 55% sucrose, $\xi = 17 \times 10^{-3}$ kg m^{-1} s^{-1}; (bottom) 1 °C in 55% sucrose, $\xi = 83 \times 10^{-3}$ kg m^{-1} s^{-1}. It is clear from the figure how the decrease of viscosity causes an increased molecular tumbling, which again causes a loss of phase coherence of the precessing nuclei. In the experiment at 1 °C, 5% free Cd was observed. This has been subtracted in the displayed perturbation function and the subtracted fraction is shown as the dashed line.

RESULTS

Structure of Metal Site in Cd-Plastocyanin. The Fourier transform of the perturbation function, $A_2G_2(t)$, collected at 1 °C from Cd-plastocyanin is shown in Figure 1. The Cd PAC spectrum of wild-type azurin (*17*) is also displayed in Figure 1 for comparison. It is seen that Cd-azurin and Cd-plastocyanin have very similar spectra with almost the same first angular frequency. The second angular frequency has, however, shifted and in the case of plastocyanin it is wider and of lower amplitude. The result of the least χ^2 fit is shown in Table 1. A comparison to the NQI of azurin (*17*) shows that the NQIs are very similar with the major difference occurring in $\omega_{\|}$ causing the shift in the second angular frequency seen in Figure 1. This similarity in the spectra shows that Cd is also coordinated to one cysteine and two histidines in plastocyanin, but the small difference in $\omega_{\|}$ corresponds to a 4° smaller His−Cd−His angle in plastocyanin than in azurin. The least χ^2 fit yielded a distribution in $\omega_{\|}$ of 2.8(1)% at 1 °C in 55% sucrose (Table 1), whereas including a distribution in $\omega_{\perp}$ did not improve the fit. A 3% Gaussian distribution in $\omega_{\|}$ corresponds to a 4° distribution in angle for one of the histidines. This angular overlap model interpretation is based on the assumption that only one of the ligands is moving and that the binding distances are unaltered.

The NQIs of Cd-plastocyanin in 55% sucrose were also measured at −11, 10, 14, and 30 °C. The parameters varied systematically from −11 to 30 °C in the following way: $\omega_{\perp}$, 0.2542(2)−0.2501(7) rad/ns; $\omega_{\|}$, 0.354(2)−0.3414(7) rad/ns; $\Delta\omega_{\|}/\omega_{\|}$, 4.4(3)−1.4(4)%; and λ, 0.0049(5)−0.019(2) ns^{-1}. The perturbation functions of plastocyanin in 55% sucrose at 1 and 30 °C are shown in Figure 2 together with the perturbation function of plastocyanin in sucrose free solution at 1 °C.

Structure of Metal Site in Ag-Plastocyanin. The NQI of ^{111}Ag-plastocyanin was determined for samples in 55% sucrose at −11, 1, 10, 20, and 30 °C. When the analysis was restricted to the part of the perturbation function collected after 17 ns after the emission of the first γ-ray, then the perturbation functions, except that collected at −11 °C, could be analyzed satisfactory with one NQI, not significantly different from the NQI of ^{111m}Cd-substituted plastocyanin. The spectrum collected at −11 °C showed, however, a significantly smaller $\omega_{\|}$ [0.313(2) rad/ns for Ag-plastocyanin compared to 0.354(2) rad/ns for Cd-plastocyanin; Table 1]. This change in $\omega_{\|}$ could also be observed in the experiments at 1, 10, 20, and 30 °C if the first 17 ns of the perturbation function were included. The reduced χ^2 could be decreased by assuming the following perturbation function:

$$G_2(t) = e^{-kt} G_2\left(\omega_{\perp}, \omega_{\|,1}, \frac{\Delta\omega_{\|}}{\omega_{\|}}, \lambda, t\right) + (1 - e^{-kt}) G_2\left(\omega_{\perp}, \omega_{\|,2}, \frac{\Delta\omega_{\|}}{\omega_{\|}}, \lambda, t\right) \quad \text{(b)}$$

The first part represents a structure related to Ag-plastocyanin

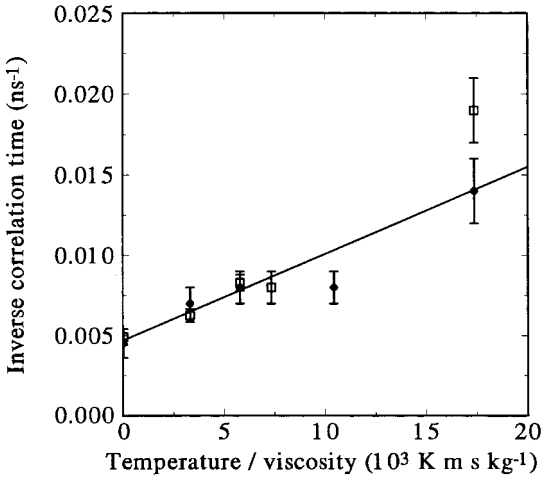

FIGURE 3: λ (inverse correlation time of rotational diffusion) as a function of absolute temperature divided by viscosity for Cd-plastocyanin (□) and Ag-plastocyanin (●). The line is the best fit to all of the shown data. The viscosity was determined by interpolation of tabulated values at 55% sucrose (*40*). The temperatures were from left to right: −11, 1, 10, 14, 20, and 30 °C. The viscosity at −11 °C was assumed to be infinite.

and the latter represents the Cd-plastocyanin structure.[2] $\omega_\perp$ was fixed to 0.254 rad/ns at all four temperatures, $\omega_{\parallel,1}$ was fixed to the value 0.313 rad/ns and $\omega_{\parallel,2}$ was fixed to the value 0.348 rad/ns, and $\Delta\omega_\parallel/\omega_\parallel$ and λ were fixed to the values obtained for the fit "after 17 ns". Thus the only free parameters are k [=ln (2)/$\tau_{1/2}$], the amplitude, and the zero level. The half-life of the structural relaxation determined this way were 15(3), 11(2), 8(2), and 8(1) ns at 1, 10, 20, and 30 °C, respectively. If the difference in $\omega_\parallel$ is ascribed to a shift in the His−metal ion−His angle, it corresponds to a 13° larger angle for Ag than for Cd. [This was calculated in a way similar to the previously used procedure (*19*).] Applying the same analysis to Ag-plastocyanin at −11 °C did not show any decay of the structure at the observable time range of approximately 100 ns.

Dynamics of the Metal Site in Cd- and Ag-Plastocyanin and in Cd-Azurin. Increasing the temperature from −11 to 30 °C lead to a decrease of $\Delta\omega_\parallel/\omega_\parallel$ from 4.4% to 1.4% and an increase in λ from 0.0049 to 0.019 ns^{-1} for Cd-plastocyanin. Both of these changes are related to the increased mobility induced by the higher temperature and in particular by the decreased viscosity. The decrease of $\Delta\omega_\parallel/\omega_\parallel$ is probably related to motional narrowing, a phenomenon well-known in NMR. The apparent rotational diffusion rates (λ) determined from the perturbation functions for Cd- and Ag-plastocyanin in 55% sucrose at different temperatures are shown in Figure 3 as a function of the temperature divided by the viscosity. This motion is due to a combined effect of internal motion (λ_0) and rotational diffusion (λ_r). The internal motion is assumed to be viscosity-independent, whereas the rotational diffusion depends linearly on the viscosity. For a rigid spherical molecule with volume V, embedded in a solution with viscosity ξ, the inverse correlation time is $\lambda_r = 1/\tau = k_BT/(\xi V)$. When the two motions are assumed to act independently in an additive way and the temperature dependence of λ_0 is neglected, then $\lambda(T/\xi) = \lambda_0 + k_BT/(\xi V)$. [This dependence of λ on T/ξ has previously been observed by PAC for ^{181}Hf-labeled transferrin (*33*).] The intersection with the ordinate in Figure 3 thus reflects the internal motion and the slope corresponds to k_B/V. λ_0 was determined to be 0.0047(4) ns^{-1} and k_B/V was determined to be [0.54(8) × 10^3] kg m^{-1} s^{-2} K^{-1}. The latter value should be compared to the calculated value of k_B/V of 0.78 × 10^3 kg m^{-1} s^{-2} K^{-1} [calculation based on a hydrated volume of 1.07 × 10^{-3} m^3/kg (*34*) and the molecular mass of plastocyanin, 10 kDa].

To compare the observed value of λ_0 to that of azurin, the rotational diffusion rate, λ, of azurin at −11 °C in 55% sucrose was determined from a ^{111m}Cd PAC spectrum collected on Cd-substituted azurin of *P. aeruginosa*. The NQI was identical to the previously observed (*17*) but the freezing of the sample lead to a larger value of $\Delta\omega_\parallel/\omega_\parallel$ of 2.6(2)% and a smaller value of λ of 0.0027(6) ns^{-1}. Assuming that the overall rotational diffusion is frozen at −11 °C in 55% sucrose but that the internal motion is unaffected, λ from this spectrum corresponds to λ_0. These data show that the internal motion of plastocyanin (λ_0 = 0.0042 ns^{-1}) is almost twice as fast as that observed for azurin (λ_0 = 0.0027 ns^{-1}), indicating that the metal site in plastocyanin is more flexible than in azurin.

Binding of Cd- and Ag-Substituted Plastocyanin to Photosystem I. When ^{111}Ag- or ^{111m}Cd-substituted plastocyanin was in aqueous solution (in the absence of sucrose) at 1 °C, the rotational diffusion rate (λ) was 0.23(2) ns^{-1} for ^{111m}Cd-plastocyanin and 0.25(5) ns^{-1} for ^{111}Ag-plastocyanin. This is of the same order of magnitude as $\omega_\parallel$ of plastocyanin (Table 1). In this case the amplitude in the perturbation function after 17 ns is zero as seen in Figure 4. When plastocyanin binds to PSI the effective molecular mass is increased, which results in a slower rotational diffusion. The NQI of ^{111}Ag-substituted plastocyanin bound to PSI was therefore determined by analyzing the perturbation function after the first 17 ns. In this way two problems were avoided: (1) a possible fraction of the plastocyanin not bound to PSI would only show up as a lack of amplitude in the analysis, and (2) the effect of the structural relaxation from Ag to Cd structure would also not interfere with the analysis. This analysis results in a λ of 0.026 ns^{-1}, which is 10 times slower than for plastocyanin not bound to PSI. The amplitude (A_2) determined from the average of two perturbation functions (one with magnesium acetate and one without) was 80% of the maximum amplitude (estimated from the average amplitude of the five perturbation functions collected at different temperatures immobilized by 55% sucrose, and with a similar sample detector geometry). This should be compared to an observed immobilized fraction of 4% (±10%) plastocyanin in the absence of PSI as well as sucrose (Table 2). Experiments were carried out in the absence of magnesium as well as in 4 mM magnesium acetate, since it is known that Mg^{2+} ions enhance the reactivity between plastocyanin and PSI (*35*). The two perturbation functions with and without magnesium acetate show a small difference

[2] It can be shown that the relaxation of one structure to another will not in general result in a simple decay of one $G_2(t)$ to another as indicated by the above equation (private communication, T. Butz). It is expected also to result in contributions to the sine part of the Fourier transform. This was not observed within the experimental uncertainty of our data (results not shown), and the reduced χ^2 from this equation was so low that we do not expect to improve the data analysis significantly by a more sophisticated model. For our purpose it is therefore sufficient to use the above equation as an approximation.

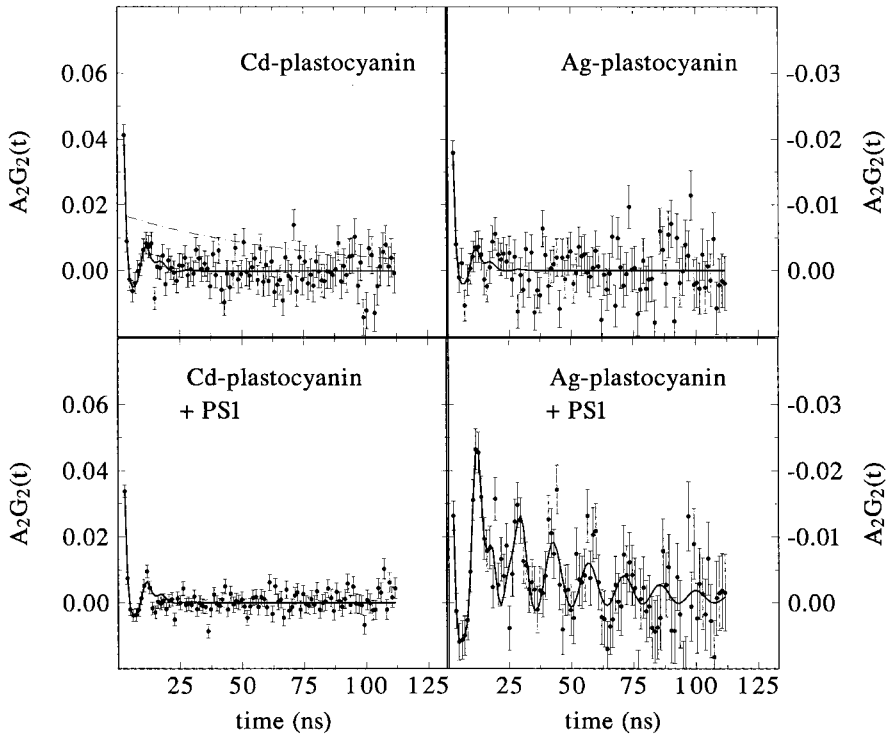

FIGURE 4: Perturbation functions of Ag- and Cd-substituted plastocyanin at 1 °C, all in the absence of sucrose, and in the absence (upper panels) and presence (lower panels) of PSI. It is clear how addition of PSI leaves the Cd perturbation function almost unaffected, whereas it causes a huge impact on the Ag perturbation function. A closer analysis shows that 4% ± 5% Cd-plastocyanin was bound to PSI, whereas 91% ± 11% Ag-plastocyanin was bound to PSI. (The first number differs from that in Table 2, because it is based on the experiment in the presence of magnesium acetate). The concentrations in the experiments including PSI were, for Ag, plastocyanin 16 μM, PSI 49 μM, and magnesium acetate 4.3 mM. For Cd the concentrations were plastocyanin 15 μM, PSI 46 μM, and magnesium acetate 4.1 mM. For Cd-plastocyanin at 1 °C, please refer to Figure 2.

Table 2: Binding of Plastocyanin to PSI under Various Conditions[a]

metal ion	plastocyanin (μM)	PSI (μM)	magnesium acetate (mM)	fraction of immobilized plastocyanin[b] (%)	K_D[c] (μM)
Ag	16	49	0	69 (±11)	22 (35−12)
Ag	16	49	4	91 (±11)	5 (12−0)
Ag[d]	15	0	4	"4 (±10)"	
Cd	15	46	0−4 (two spectra)	9 (±6)	470 (260−1500)

[a] The temperature was 1 °C, the pH was 7.5, and the buffer was 24.2 and 28 mM Hepes. The detergent was 0.2% decyl maltoside. No nonradioactive Cd nor Ag was added. [b] This was determined from the amplitude of the perturbation function omitting the first 17 ns from the data analysis. [c] K_D was calculated with the assumption that apoplastocyanin did not bind to PSI and the fact that the concentration of radioactively labeled plastocyanin is insignificant compared to the PSI concentrations. The numbers in parentheses gives the range given by 1 standard deviation in fraction bound. [d] This sample, which contained neither sucrose nor PSI, is included for comparison.

in amplitude corresponding to a change in the fraction of bound plastocyanin from about 69% (±11%) for the experiment without magnesium acetate to about 91% (±11%) for the experiment with magnesium acetate. The corresponding dissociation constants are 5 μM for the sample containing magnesium acetate and 22 μM for the sample without magnesium acetate (see Table 2).

For ^{111m}Cd-substituted plastocyanin, we were unable to monitor any binding to PSI by fitting all the different NQI parameters to the perturbation function. If however, the parameters determined for Ag-plastocyanin bound to PSI are used for analyzing the spectra, and the data analysis is limited to the perturbation function after 17 ns, then the amplitudes (A_2) correspond to a fraction of plastocyanin bound to PSI of 9% (±6%) for the average of two spectra, one with and one without magnesium acetate, corresponding to a dissociation constant of 470 μM (note the large uncertainty in the latter number, Table 2). The ratio between the two dissociation constants K_D^I/K_D^{II} is 0.010 ± 0.016 (where the uncertainty has been derived by propagation of error). This results in $24 < K_D^{II}/K_D^I < \infty$, with 95% confidence.

Metal Site Structure of Ag-Plastocyanin Bound to PSI. In Table 1 the NQI values of Ag-plastocyanin bound to PSI, Ag-plastocyanin at −11 °C, and Ag-plastocyanin at 1 °C after the relaxation are listed. The difference between $\omega_{||}$ of frozen Ag-plastocyanin and $\omega_{||}$ of Cd-plastocyanin is 0.031 rad/ns; this is significant (in terms of experimental uncertainty) and it is too large to be explained by second coordination sphere changes only. It is therefore interpreted as a change of the metal site conformation (vide ante). In contrast to this, the difference between the NQI of frozen Ag-plastocyanin and Ag-plastocyanin binding to PSI is within the experimental uncertainty. Since no relaxation of the NQI of Ag-plastocyanin bound to PSI could be observed on the time scale of about 100 ns, this means that the binding of Ag-plastocyanin to PSI has stabilized the metal site in a conformation that is structurally similar to that of frozen Ag-plastocyanin.

DISCUSSION

The binding of plastocyanin to PSI as a function of the charge state of the copper ion is an important part of the electron transport in photosynthesis and has previously been studied by observing the absorbance changes of P700 after photooxidation induced by a laser flash (*8*). In the present study the binding is monitored through the rotational diffusion of plastocyanin and, to our knowledge, this is the first application of PAC spectroscopy to the study of protein−protein interaction. It further focuses on the role of the structure of the metal site in contributing to the regulation of the reduction potential of plastocyanin for bound and free plastocyanin, respectively. The dissociation constant was here found to depend strongly on the metal ion. K_D^{II}/K_D^{I} is at least 24, which corresponds to a difference in binding energy of k_BT ln (K_D^{II}/K_D^{I}) = 75 meV. It is shown in the work by Drepper et al. (*8*) (see the introduction) that the dissociation constant depends on the charge of the metal ion of plastocyanin for Cu(I)/Cu(II). Together with the present results, based on direct determination of dissociation constants, this indicates that the driving force in the complex is significantly different from what is obtained by the difference in the two reduction potentials of free plastocyanin and free P700. However, it should be noted that the difference in binding energy for Cd- and Ag-plastocyanin to reduced P700 cannot directly be related to the driving force in the natural complex between plastocyanin and P700. The reason is 2-fold: first, the substituting metal ions are not identical to the native Cu(I)/Cu(II), and second, the binding of Ag-plastocyanin to oxidized P700 has not yet been measured.

The present work also shows a difference between the structure of Cd- and Ag-plastocyanin in solution and, further, that when Ag-plastocyanin is bound to PSI, the Ag structure is stabilized. The well-defined effect of the binding on the structure of the metal site indicates that Ag-plastocyanin binds to a specific site on PSI, most probably the functional site for the electron transfer. This suggests that the metal site structure is involved in regulating the dissociation constant of plastocyanin to PSI in addition to the charge−charge interactions between the two proteins suggested by Drepper et al. (*8*).

Structure of Metal Site in Cd-Plastocyanin. When the PAC spectrum of Cd-plastocyanin is compared to the PAC spectrum of Cd-azurin (Figure 1), the first thing one notices is the high similarity, indicating that the metal site structures of Cd-plastocyanin and Cd-azurin are similar, in accordance with the similarity between the Cu(II) structures based on X-ray diffraction (*14*, *20*). Second, one notices a significant broadening of the second angular frequency for Cd-plastocyanin. As described in the Results section, this can be related to an in-plane distribution of the position of one of the ligands. Also, the high apparent rotational diffusion at infinite viscosity (here obtained by freezing to −11 °C in 55% sucrose) indicates a high degree of flexibility of the metal site in plastocyanin. If one assumes that this flexibility reflects the motion of one of the ligands, then the flexible ligand is unlikely to be the cysteine. The reason for this is that moving the cysteine in the plane will increase one of the Cys−metal ion−His angles, whereas the other is decreased and the combined effect on the PAC spectrum is very small. Thus if only one of the ligands is involved in forming the unusual line width, it must be one of the two histidines having an in-plane distribution of positions with a standard deviation of approximately 4°. PAC alone cannot distinguish between the two histidines, but the most likely candidate is His87, which is known to become protonated and rotate 180° about the $C^{\beta}-C^{\gamma}$ bond at low pH for reduced [Cu(I)] plastocyanin (*16*). This interpretation is based on the assumption that only one of the coordinating amino acids is moving. Other possible interpretations could involve several ligands, and/or the metal ion itself, and might explain the residual electron density observed around the copper ion by X-ray crystallography (*15*).

Structure of Metal Site in Ag-Plastocyanin. The perturbation functions of Ag-plastocyanin are well described as an NQI of Ag-plastocyanin with a smaller value of $\omega_{||}$ (0.313 rad/ns) compared to Cd-plastocyanin (Table 1). In the unfrozen samples this structure is relaxing rapidly into the NQI characteristic of Cd-plastocyanin with a half-life between 15 and 8 ns depending on the temperature, but the binding of Ag-plastocyanin to PSI prevents this relaxation from taking place on a time scale of 100 ns. The structural interpretation of this is that one of the histidines (presumably His87) takes on a different position for Ag-plastocyanin than for Cd-plastocyanin but that this difference relaxes fast after the decay of Ag to Cd. That the structural difference involves His87 is also supported by the stabilization of the Ag geometry by the binding to PSI, since this amino acid is part of the hydrophobic patch involved in the binding to PSI. The corresponding difference in N−metal ion−N angle between Cd and Ag is approximately 13°. Motion of His87 is the simplest model explaining these data; however, the conformational difference could also involve more ligands and/or the metal ion itself. It is important to note that the difference in the spectra between Ag and Cd is not due to a partial protonation of the Nδ of His87. If this nitrogen is protonated and the metal ion relaxes to the plane of Met92, Cys84, and His37 [as is the case for Cu(I)-plastocyanin at low pH; see the introduction], then this conformation would have the $\omega_{\perp}$ characteristic of these three ligands and would be observed as a shift of the first angular frequency.

Relationship between Flexibility of Cd Metal Site and Difference between Ag and Cd Structures. To compare the flexibility of the Cd metal site and the structural difference between Cd- and Ag-plastocyanin in a quantitative way, we will ignore the changes in charge−charge interactions between plastocyanin and PSI. We will assume that all of the increase of the dissociation constant for Cd-plastocyanin to PSI compared to Ag-plastocyanin to PSI is due to a conformation of plastocyanin bound to PSI that is favorable for Ag-plastocyanin but not for Cd-plastocyanin. If we further parametrize the conformational energy of the metal site by the His−Cd−His angle, α, and assume that this energy depends on the angle as a harmonic oscillator, then we get $\Delta G = {}^1/_2 k(\alpha - \alpha_0)^2$, where α_0 is the equilibrium value for Cd. The difference in binding energy, k_BT ln (K_D^{II}/K_D^{I}), of at least 75 meV must then correspond to the increase in energy of the Cd site by forcing it into the Ag conformation and suggests that ΔG = 75 meV (or more) for $\alpha - \alpha_0$ = 13° (from this k can be determined). This together with the Boltzmann distribution yields a probability density of α:

$$p(\alpha) = \exp(-\Delta G/k_B T) = \exp(-{}^1/_2(\alpha - \alpha_0)^2/\sigma^2)$$

where $\sigma^2 = k/k_B T$. The value of σ derived from this Gaussian distribution with a temperature of 274 K is 5°. This is very close to the angular distribution with standard deviation 4° derived from the unusual frequency distribution of Cd-plastocyanin, which affects only the second and the third angular frequencies. To make this comparison we ignored the charge−charge interaction and we used the lower limit of 75 meV for ΔG. Therefore we do not wish to emphasize the numbers but rather to draw attention to the relationship between (1) assuming that the binding of plastocyanin is partly regulated by the position of the His87 and (2) the distribution of the position of His87 for plastocyanin in solution.

Comparison to Crystal Structures. The crystal structure of oxidized poplar plastocyanin has been known since 1983 (*14*) and for reduced poplar plastocyanin since 1986 (*16*), while the structure of oxidized spinach plastocyanin recently was determined for the Gly8Asp mutant (*15*). The structure of the (oxidized) copper site showed no significant difference for spinach plastocyanin compared to poplar plastocyanin. The largest differences between the two copper sites occurred in the distances between the copper ion and the two coordinating $N^{\delta 1}$ atoms of His37 (0.11 Å) and His87 (0.16 Å). We will for simplicity only refer to the poplar structures (*14*, *16*) in the following discussion. The major difference between the structure of oxidized poplar plastocyanin and the structure of reduced poplar plastocyanin at pH 7.8 is a shift of the copper ion out of the plane (about 0.1 Å) for the reduced plastocyanin. Such a displacement is not observed for ^{111}Ag-plastocyanin compared to ^{111}Cd-plastocyanin since the first angular frequency is identical for the two PAC spectra. This does not mean, however, that Ag is not shifted out of the plane, as is Cu(I), but only that such a possible shift must have relaxed within less than a few nanoseconds after the decay from Ag to Cd, in which case it would be unobservable by PAC.

The comparison of the two copper structures, Cu(I) at pH 7.8 (*16*) and Cu(II) at pH 6 (*14*), does not indicate that the position of one of the histidines is shifted as observed with Ag PAC. However, for Cu(I)plastocyanin at pH 7.0 (*16*) there is an increased distance of 3.44 Å between the two coordinating nitrogens compared to 2.97 Å for Cu(II)-plastocyanin at pH 6 (*14*). This is interesting because the protonation of His87 seems to take place between pH 5.1 and 5.9, based on the average distance of the copper ion to the plane formed by N(His37), S(Cys84), and S(Met92). We will therefore use the Cu(I)plastocyanin structure at pH 7.0 for the comparison. If we further assume that by PAC we observe the geometry of the monovalent ion after it has relaxed to the plane, then an increase of the N−N distance from 2.97 Å for Cu(II)-plastocyanin to 3.44 Å for Cu(I)-plastocyanin corresponds to an increase in N−Cu−N angle by approximately 15°. The increased distance between the two histidines is thus in very good agreement with the increased angle observed for Ag PAC compared to Cd PAC.

Strict Complementarity in the Interaction between the Two Proteins. The observation that the binding of plastocyanin to PSI forces a metal site structure that favors the Ag structure also suggests that a strong binding between the two proteins requires a strict complementarity between the two protein surfaces. Other observations support this requirement: The *B*-factors of spinach plastocyanin obtained by X-ray crystallography are low at the hydrophobic surface surrounding His87, meaning that plastocyanin is quite rigid in this region (*15*). Second, even rather small changes in the hydrophobic patch induced by a mutation drastically lower the binding capability to PSI. Examples of this are the loss of the fast phase when Leu12 is replaced by Glu, Ala, or Asn (*4*) and the very small amplitude of the fast phase for the Pro36Gly mutant (*2*). Similar changes have been observed for the Gly10Leu and Ala90Leu mutants (*36*). A factor of at least 24 in the dissociation constants might seem large, but the corresponding difference in binding energy of 75 meV (7.2 kJ mol^{-1}) is not more than the typical energy of a hydrogen bond. The observation that the Ag structure is immobilized at −11 °C in 55% sucrose supports the hypothesis that the structural difference also involves the surface of plastocyanin.

PERSPECTIVE

Though PAC spectroscopy directly provides a means of measuring the binding of a small molecule to a larger molecule through rotational diffusion, PAC alone can only provide information about the molecular mechanism behind the binding if that involves the very close vicinity of the PAC probe. In the present case a large difference in dissociation constant was found for plastocyanin containing divalent Cd and plastocyanin containing monovalent Ag (in accordance with what is attractive from a biological function point of view). At the same time a geometrical difference at the metal site is observed for the two different metal ions. This geometrical difference relaxes for Ag-plastocyanin in solution when Ag decays to Cd but is stabilized if Ag-plastocyanin is bound to PSI. This suggests that the structural difference of the metal site is also involved in the molecular mechanism behind the difference in binding constants. Though it remains to be shown whether the copper protein undergoes the same structural changes, the present study gives a hint to the mechanism that might be behind the regulation of the binding to PSI as a function of the redox state of the native copper protein. If the present findings are transferred to the native system, they suggest the following series of events:

First, reduced plastocyanin binds to PSI. In this state the Cu(I) ion is displaced out of the plane and the distance between the two coordinating nitrogens is large.

Second, the electron is transferred to PSI and the nucleus might quickly relax closer to the plane (this relaxation is too fast to be observed by PAC at temperatures close to 0 °C.) At a slower time scale the distance between the two coordinating nitrogens is decreased (PAC suggests that for plastocyanin in solution this structural relaxation takes place at a time scale of 10 ns but that it is slowed by the binding of plastocyanin to PSI). This destroys the close structural match between the two protein surfaces, and this together with the change in the Coulomb interaction weakens the binding between plastocyanin and PSI.

Third, the now oxidized plastocyanin leaves PSI. The rate constant of this, k_{off}^{II}, is on the order of 9×10^3 s^{-1} (*8*). The PAC experiments only indicate that it is slower than 40 ns,

judged from the fact that Ag-plastocyanin does show slow rotational diffusion even though Ag has decayed to Cd.

This scheme of events also suggests future experiments: The p*K* of the protonation of His87 could be monitored by Ag PAC in the absence and in the presence of PSI. This would directly reveal whether the binding of plastocyanin to PSI affects this p*K* and/or whether protonation of His87 affects the binding of plastocyanin to PSI. The method could further be used to study the binding of Ag-plastocyanin to oxidized PSI. Such a study could give the dissociation constant missing in order to compare the differences in binding energies with respect to the driving force.

It seems likely that a mechanism similar to that observed in the present study is involved in plastocyanin binding to cytochrome *f*. Here the binding of plastocyanin to cytochrome *f* results in a lowering of the reduction potential of plastocyanin by 30 mV (*37*). Thus the analogy would suggest that the binding of plastocyanin to cytochrome *f* favors the structure of the oxidized plastocyanin. A similar mechanism seems to regulate the electron transfer between amicyanin and methylamine dehydrogenase, which also cannot be explained by a simple theory (*38*). For this redox couple a recent investigation has shown that the binding of reduced amicyanin to methylamine dehydrogenase stabilizes the conformation of His-95, to the position where it is bound to the copper ion (*39*). For amicyanin not bound to methylamine dehydrogenase this conformation is found in the oxidized protein, but in the reduced protein the histidine can protonate and "flip" in a way very similar to that of plastocyanin but with a p*K* of about 7.5. This binding between the two redox partners lowered the reduction potential of amicyanin by 73 mV (*39*). On the basis of the PAC experiments it seems likely that what has previously been interpreted as a conformational rearrangement of the plastocyanin−PSI complex prior to the electron transfer is at least partly due to a decreased driving force and a change of conformation in plastocyanin after the electron transfer.

ACKNOWLEDGMENT

We are indebted to Marianne Lund Jensen and Hanne Linde Nielsen for excellent help with sample preparations and to Simon Young and Mikael Ejdebäck for cultivating and purifying plastocyanin.

REFERENCES

1. Young, S., Sigfridsson, K., Olesen, K., and Hansson, Ö. (1997) *Biochim. Biophys. Acta 1322*, 106−114.
2. Sigfridsson, K., Young, S., and Hansson, Ö. (1997) *Eur. J. Biochem. 245*, 805−812.
3. Sigfridsson, K., He, S. P., Modi, S., Bendall, D. S., Gray, J., and Hansson, Ö. (1996) *Photosynth. Res. 50*, 11−21.
4. Sigfridsson, K., Young, S., and Hansson, Ö. (1996) *Biochemistry 35*, 1249−1257.
5. Hervas, M., Navarro, J. A., Diaz, A., Bottin, H., and Delarosa, M. A. (1995) *Biochemistry 34*, 11321−11326.
6. Bottin, H., and Mathis, P. (1985) *Biochemistry 24*, 6453−6460.
7. Bottin, H., and Mathis, P. (1987) *Biochim. Biophys. Acta 892*, 91−98.
8. Drepper, F., Hippler, M., Nitschke, W., and Haehnel, W. (1996) *Biochemistry 35*, 1282−1295.
9. Nordling, M., Sigfridsson, K., Young, S., Lundberg, L. G., and Hansson, O. (1991) *FEBS Lett. 291*, 327−330.
10. Butz, T. (1989) *Hyperfine Interact. 52*, 189−228; Erratum (1992) *Hyperfine Interact. 73*, 387.
11. Frauenfelder, H., and Steffen, R. M. (1965) *Alpha-, Beta-, Gamma-ray Spectroscopy* (Siegbahn, K., Ed.) Vol. 2, pp 97−1198, North-Holland, Amsterdam.
12. Bauer, R. (1985) *Q. Rev. Biophys. 18 (1)*, 1−64.
13. Bauer, R., Bjerrum, M. J., Danielsen, E., and Kofod, P. (1991) *Acta Chem. Scand. 45*, 593−603.
14. Guss, J. M., and Freeman, H. C. (1983) *J. Mol. Biol. 160*, 521−563.
15. Xue, Y., Ökvist, M., Hansson, Ö., and Young, S. (1998) *Protein Sci. 10*, 2099−2105.
16. Guss, J. M., Harrowell, P. R., Murata, M., Norris, V. A., and Freeman, H. C. (1986) *J. Mol. Biol. 192*, 361−387.
17. Danielsen, E., Bauer, R., Hemmingsen, L., Andersen, M., Bjerrum, M. J., Butz, T., Tröger, W., Canters, G. W., Hoitink, C. W. G., Hansson, Ö., and Messerschmidt, A. (1995) *J. Biol. Chem. 270*, 573−580.
18. Danielsen, E., Bauer, R., Hemmingsen, L., Bjerrum, M. J., Butz, T., Tröger, W., Canters, G. W., den Blaauwen, T., and van Pouderoyen, G. (1995) *Eur. J. Biochem. 233*, 554−560.
19. Bauer, R., Danielsen, E., Hemmingsen, L., Bjerrum, M. J., Hansson, Ö., and Singh, K. (1997) *J. Am. Chem. Soc. 119*, 157−163.
20. Nar, H., Messerschmidt, A., Hubert, R., van de Kamp, M., and Canters, G., W. (1991) *J. Mol. Biol. 221*, 765−772.
21. Nar, H. (1992) Ph.D. Thesis, Technical University München, Germany.
22. Tröger, W., Lippert, C., Sigfridsson, K., Hansson, Ö., McLaughlin, E., Bauer, R., Danielsen, E., Hemmingsen, L., Bjerrum, M. J., and the ISOLDE Collaboration (1996) *Z. Naturforsch. 51a*, 431−436.
23. Danielsen, E., Kroes, S. J., Canters, G. W., Bauer, R., Hemmingsen, L., Singh, K., and Messerschimdt, A. (1997) *Eur. J. Biochem. 250*, 249−259.
24. Andersen, B., Koch, B., and Scheller, H. V. (1992) *Physiol. Plant. 84*, 154−161.
25. Naver, H., Scott, M. P., Golbeck, J. H., Moller, B. L., and Scheller, H. V. (1996) *J. Biol. Chem. 271*, 8996−9001.
26. Tjus, S. E., Møller, B. L., and Scheller, H. V. (1998) *Plant Physiol. 116*, 755−764.
27. Arnon, D. I. (1949) *Plant Physiol. 24*, 1−15.
28. Ejdebäck, M., Young, S., Samuelsson, A., and Karlsson, B. G. (1997) *Protein. Expression Purif. 11*, 17−25.
29. Butz, T., Saibene, S., Fraenzke, T., and Weber, M. (1989) *Nuclear Instrum. Methods Phys. Res. A284*, 417−421.
30. Bauer, R., Danielsen, E., Hemmingsen, L., Sørensen, M. V., Ulstrup, J., Friis, E. P., Auld, D. S., and Bjerrum, M. J. (1997) *Biochemistry 36*, 11514−11524.
31. Danielsen, E., and Bauer, R. (1990) *Hyp. Int. 62*, 311−324.
32. Haas, H., and Shirley, D. A. (1973) *J. Chem. Phys. 58*, 3339−3359.
33. Schwab, F. J., Appel, H., Neu, M., and Thies, W. G. (1992) *Eur. Biophys. J. 21*, 147−154.
34. Kuntz, I. D., and Kauzmann, W. (1974) *Adv. Protein Chem. 28*, 239−345
35. Lockau, W. (1979) *Eur. J. Biochem. 94*, 365−373.
36. Haehnel, W., Jansen, T., Gause, K., Klösgen, R. B., Stahl, B., Michl, D., Huvermann. B., Karas, M., and Herrmann, R. G. (1994) *EMBO J. 13*, 1028−1038.
37. Malkin, R., Knaff, D. B., and Bearden, A. J. (1973) *Biochim. Biophys. Acta 305*, 675−678.
38. Brooks, H. B., and Davidson, V. L. (1994) *Biochemistry 33*, 5696−5701.
39. Zhu, Z., Cunane, L. M., Chen, Z., Durley, R. C. E., Mathews, F. S., and Davidson, V. L. (1998) *Biochemistry 37* (49), 17128−17136.
40. Fasman, G. D., Ed. (1976) *CRC Handbook of Biochemistry and Molecular Biology*, 3rd edition, Physical and Chemical Data, Volume I, CRC Press, Cleveland, OH.

BI990869Y